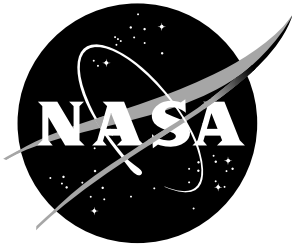


NASA/TM-2020-220560



Evaluation of Packing_3D Code for Design of Variable-Depth, Bent-Chamber Acoustic Liners

*Miroslava M. Marinova, Michael G. Jones, and Noah H. Schiller
Langley Research Center, Hampton, Virginia*

February 2020

NASA STI Program... in Profile

Since its founding, NASA has been dedicated to the advancement of aeronautics and space science. The NASA scientific and technical information (STI) program plays a key part in helping NASA maintain this important role.

The NASA STI Program operates under the auspices of the Agency Chief Information Officer. It collects, organizes, provides for archiving, and disseminates NASA's STI. The NASA STI Program provides access to the NASA Aeronautics and Space Database and its public interface, the NASA Technical Report Server, thus providing one of the largest collections of aeronautical and space science STI in the world. Results are published in both non-NASA channels and by NASA in the NASA STI Report Series, which includes the following report types:

- **TECHNICAL PUBLICATION.** Reports of completed research or a major significant phase of research that present the results of NASA programs and include extensive data or theoretical analysis. Includes compilations of significant scientific and technical data and information deemed to be of continuing reference value. NASA counterpart of peer-reviewed formal professional papers, but having less stringent limitations on manuscript length and extent of graphic presentations.
- **TECHNICAL MEMORANDUM.** Scientific and technical findings that are preliminary or of specialized interest, e.g., quick release reports, working papers, and bibliographies that contain minimal annotation. Does not contain extensive analysis.
- **CONTRACTOR REPORT.** Scientific and technical findings by NASA-sponsored contractors and grantees.

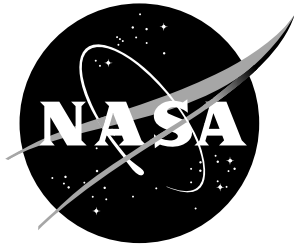
- **CONFERENCE PUBLICATION.** Collected papers from scientific and technical conferences, symposia, seminars, or other meetings sponsored or co-sponsored by NASA.
- **SPECIAL PUBLICATION.** Scientific, technical, or historical information from NASA programs, projects, and missions, often concerned with subjects having substantial public interest.
- **TECHNICAL TRANSLATION.** English-language translations of foreign scientific and technical material pertinent to NASA's mission.

Specialized services also include organizing and publishing research results, distributing specialized research announcements and feeds, providing information desk and personal search support, and enabling data exchange services.

For more information about the NASA STI Program, see the following:

- Access the NASA STI program home page at <http://www.sti.nasa.gov>
- E-mail your question to help@sti.nasa.gov
- Phone the NASA STI Information Desk at 757-864-9658
- Write to:
NASA STI Information Desk
Mail Stop 148
NASA Langley Research Center
Hampton, VA 23681-2199

NASA/TM-2020-220560



Evaluation of Packing_3D Code for Design of Variable-Depth, Bent-Chamber Acoustic Liners

*Miroslava M. Marinova, Michael G. Jones, and Noah H. Schiller
Langley Research Center, Hampton, Virginia*

National Aeronautics and
Space Administration

Langley Research Center
Hampton, Virginia 23681-2199

February 2020

The use of trademarks or names of manufacturers in this report is for accurate reporting and does not constitute an official endorsement, either expressed or implied, of such products or manufacturers by the National Aeronautics and Space Administration.

Available from:

NASA STI Program / Mail Stop 148
NASA Langley Research Center
Hampton, VA 23681-2199
Fax: 757-864-6500

Abstract

Increases in the bypass ratio for commercial aircraft engines have caused the broadband fan noise component to become dominant. As a result, there is a need to develop improved acoustic liners suitable for absorption of this fan noise over a wide frequency range, preferably up to at least two octaves. Variable depth liners with bent chambers and three-dimensional geometries present one way to achieve this goal, however, they can be difficult and time-consuming to design due to their complexity and volume constraints. A packing code, called Packing3D, has been developed that automatically designs the chamber configurations of such liners once the chamber dimensions and volume constraints are known. The code uses a randomized trial and error approach to place each chamber in a representation of the liner sample, then returns a colored diagram and sufficient information for the liner sample to be fabricated. For evaluation, the code is used to design four liner samples of varying levels of complexity. These samples are tested with and without a mesh facesheet in the NASA Langley Normal Incidence Tube, and the results are compared to predictions computed in COMSOL. The results indicate that the packing code is able to quickly design samples that are predictable, achieve the desired absorption spectrum, fit the given constraints, and are able to be built. This code is flexible, lends itself to optimization, and allows samples to be designed quickly, accurately, and efficiently.

1 Introduction

One of the more significant contributors to commercial aircraft noise is the rotating fan [1]. Acoustic liners installed in the walls of the inlet and aft bypass duct of engine nacelles are used to reduce fan noise before it radiates to the communities surrounding airports. Conventional, single-degree-of-freedom liners (SDOF, see Fig. 1) are comprised of multiple resonant chambers packaged between a rigid backplate and a perforated facesheet. The chamber length is the main factor that determines its resonant frequency, which in turn determines the frequency of sound that it can best attenuate. Since all of the chambers of an SDOF liner are identical, these liners were excellent for reduction of tonal fan noise generated by early commercial aircraft engines.

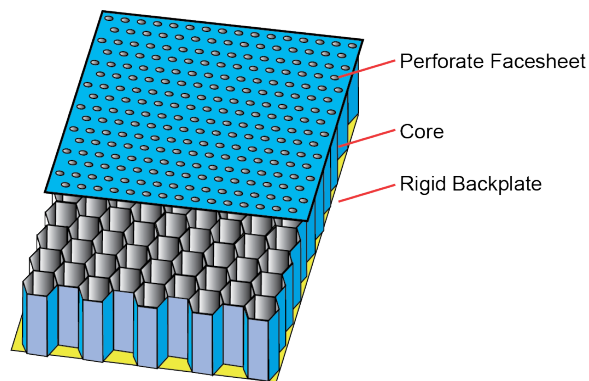


Figure 1: Sketch of single-degree-of-freedom acoustic liner.

However, continued increases in engine bypass ratio have caused the broadband component to become more dominant. Corresponding growth of the fan diameter has also resulted in lower fan

speeds, causing an increase in low-frequency noise. A number of liner configurations have been explored to address this change in the character of fan noise. One such concept that has been explored by the NASA Langley Research Center liner physics team is the variable-depth liner [2, 3]. Variable-depth liners have chambers of uniform cross-sectional area, but, unlike in traditional liners, each chamber may have a different length. These distinct chamber lengths allow these liners to attenuate noise at a number of distinct frequencies, and this combination of tuning frequencies causes the variable-depth liner to efficiently absorb fan noise over a broad range of frequencies [3]. In order to extend this frequency range to lower frequencies, a portion of these chambers must be lengthened to such an extent as to require those chambers to be bent in order to fit in the available volume. The main purpose of this paper is to present a packaging code that has been implemented to aid in the chamber arrangement step in the design of these variable-depth, bent-chamber acoustic liners.

To achieve the desired acoustical properties, the appropriate number and dimensions of the chambers in a liner sample must be chosen. Once these factors are determined, the chambers must be packaged to fit within the sample (oriented within the given volume). The chambers can be bent in any direction within the liner. The bends are assumed to have minimal impact on the acoustic performance as long as the length of individual chambers (measured along the center of the chambers) remains constant [3]. This property allows the chambers to be packaged tightly and the volume of the liner to be used efficiently.

The packaging step can be very time consuming and inefficient if done by hand, especially if there are a large number of chambers or stringent constraints on liner size. The Packing3D MATLAB code is meant to streamline this process by automating the packaging stage of design. The code fits chambers of a known length into a known volume, changing the shape of the chambers as necessary. If the dimensions of the desired liner sample and the dimensions of the chambers to be placed are known, the Packing3D code can produce a diagram depicting a possible arrangement of chambers in the given volume. This is done by dividing the available volume into cells and randomly placing the chamber cell by cell until all chambers are placed or the volume is filled. This method was chosen because it is simple, requires little computation, and lends itself to optimization. The packaging process can be completed in seconds and the end result contains sufficient information for the sample to be built.

Four liner samples were created to test this code. The number and overall lengths of the chambers were determined iteratively, using an impedance model to predict the acoustic performance of the sample. The Packing3D code was then used to package the chambers and provide the final sample designs. The samples were built from these designs and tested in the NASA Langley Normal Incidence Tube (NIT). The measured impedances are compared with those predicted using a COMSOL numerical model to verify the ability of the code to accurately design a liner sample with the desired characteristics.

The Packing3D code saves time, decreases the risk of calculation errors, and automatically produces a visual output that can be used to easily communicate the design to the manufacturer. This code can be used for any number of chambers at any number of different chamber lengths and allows for three-dimensional geometries in order to use the allotted volume more efficiently. While earlier bent-chamber configurations have typically been restricted to two-dimensional designs, this code incorporates the ability to bend chambers at right angles in any direction. These capabilities are especially beneficial in circumstances when space for the liner is limited or a large number of chambers must be placed in a complex arrangement.

Section 2 provides a description of the algorithm used in the packing code. Section 3 presents a brief overview of the analytic impedance model used to determine the chamber depths and the numerical COMSOL model used to evaluate the final configurations. Some representative results are provided in Section 4, and key features are summarized in Section 5.

2 Algorithm

Figure 2 provides a flowchart description of the Packing3D algorithm used to design bent-chamber, variable-depth acoustic liners. It is assumed that key geometric features of the liner are known a priori. These include the desired depth of the full liner sample and the minimum width of the walls (partitions) separating the chambers. The user must also know the width of the chamber cross-sections as well as the length and number of chambers to be packaged. The current version of the code assumes that the design is for an NIT sample, which has a two-inch by two-inch horizontal cross-section. Each chamber is assumed to have a square cross-section, which is assumed to be of proper width to fit within the dimensions of an NIT sample. The code allows the chambers to be bent at right angles in any direction, but the user chooses the sequence in which the code will attempt to place the chambers in the sample, as this has an impact on the final design. The user may also choose if they would like to watch as the chambers are placed or simply view the final design.

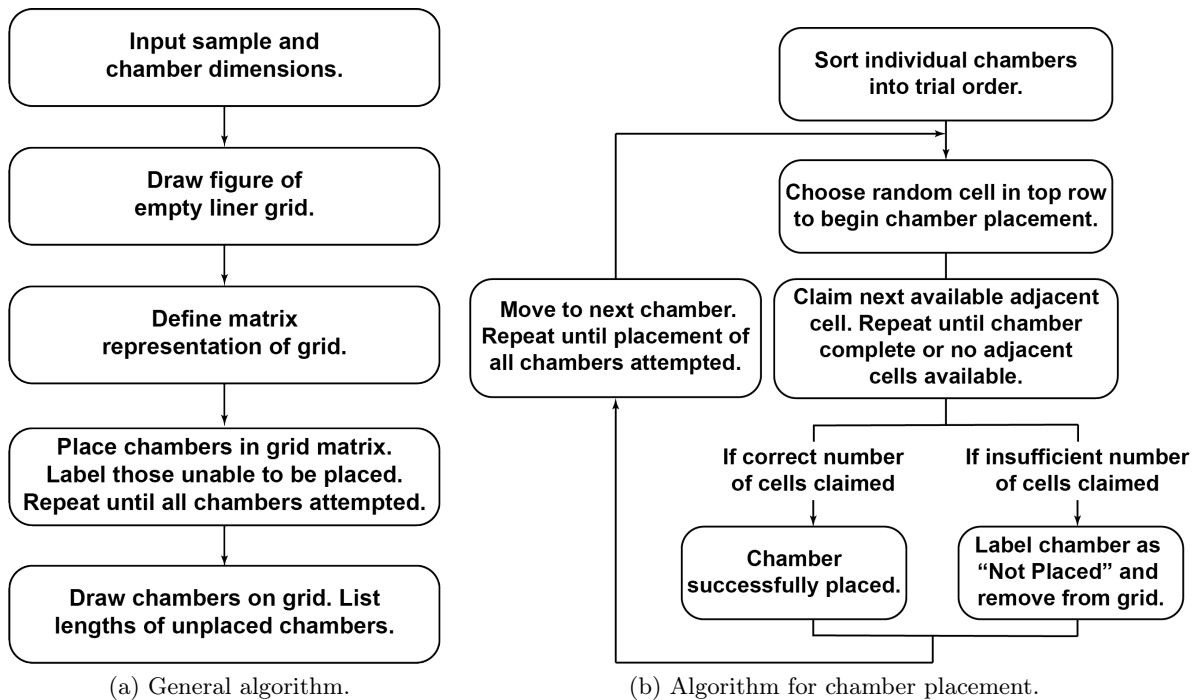


Figure 2: Packing3D algorithm.

At the start of the process, a grid representing the sample is drawn in a figure window. This corresponds to the given dimensions and represents the solid sample divided into a grid of cells to aid chamber placement. Each cell is cubic, with a side length equal to the combined width of a chamber

and a wall. The only exception to this is that the top cell (closest to the surface) may be vertically longer than the rest in order to achieve the desired sample total depth. A three-dimensional matrix representing the grid is created, where each cell is represented by row, column, and slice coordinates (r,c,s). A zero in the matrix indicates that the cell is available and a one indicates that it is occupied. Figure 3 shows an example of a grid with five rows, five columns, and five slices.

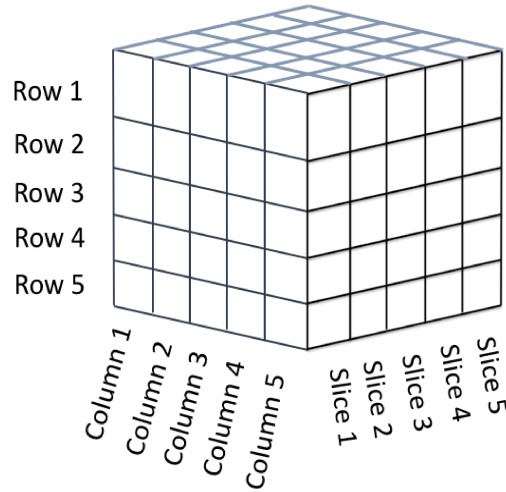


Figure 3: Grid of cells used by Packing3D to facilitate liner design. Each cell is represented by a number in a three-dimensional matrix.

Each individual chamber is identified by its length (two chambers of the same length initially have identical identifiers). The chambers are separated into “bins” and sorted into the order in which the code will attempt to place them. A random cell in the top row is chosen as a starting point for the first chamber. The chamber then claims adjacent cells until it occupies enough to contain its full length. Adjacent cells include those immediately below, to the left, to the right, or above the previous cell. If these are all occupied, the chamber may also claim cells in the next slice or the previous slice (moving “forward” or “backward”). This placement pattern ensures that the geometry of the chamber remains in as few dimensions as possible, keeping within the plane of a slice unless forced to bend in the normal direction.

When a cell is claimed, the corresponding zero in the grid matrix is replaced with a one to signal that it is occupied and its placement information is stored in the “bin” of that particular chamber. This placement information includes the coordinates of the claimed cell, the direction in which the chamber has stepped, and the amount of chamber length remaining to be placed. The unoccupied space remaining in the last cell claimed by the chamber is also recorded. If a chamber cannot be placed (the number of available adjacent cells is insufficient), it is labelled as “Not Placed” and its placement information is reset. These steps are repeated until all chambers have been placed or reset.

The element of randomness in the first step of the placement of each chamber allows for a different configuration on each iteration. For this reason, the placement is repeated to find a “best” solution (as many chambers placed as possible in the given volume). The placement information of each chamber is then used to draw the chamber onto the empty sample grid created at the

beginning. The final representation contains sufficient geometry information for the sample to be manufactured.

Figures 4 - 7 show the designs of the samples used in this study; they represent a typical output of the Packing3D code. Each slice is drawn to scale, with the chambers and walls between them depicted. The chamber colors are used to aid readability and do not correspond to the lengths of the chambers. Slices are separated by a “wall” just as the chambers are and each slice is assumed to have a thickness equal to the width of a cell. A circle signifies that a chamber continues out of the page into the previous slice and a cross signifies that a chamber continues into the page to the next slice. The chambers that have not been placed are listed by length in the order in which their placement was attempted. If nothing is listed under “Not Placed,” this is an indication that all chambers were successfully arranged in the given volume. All measurements are in inches. Additionally, the variable labelled “Best” contains all of the information depicted in Figures 4 - 7, as well as the amount of unused space in any partially filled cells. The last quantity is often necessary information for the sample to be built.

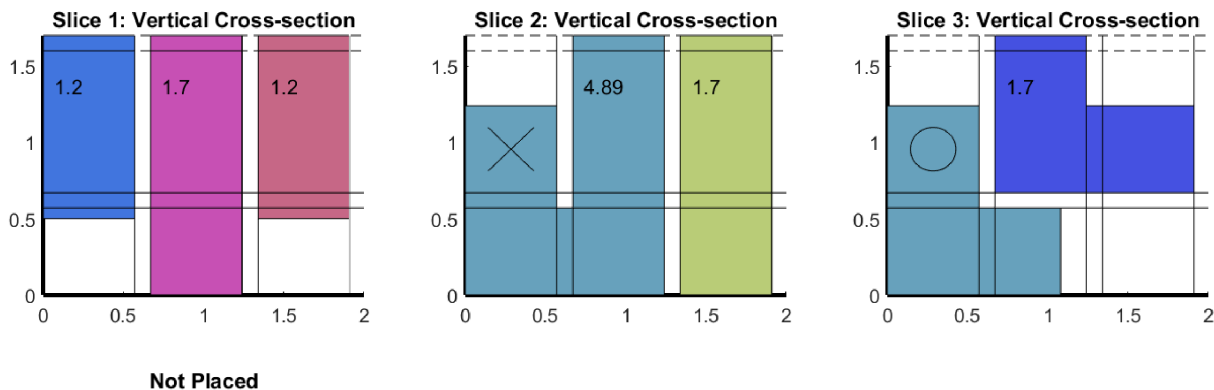


Figure 4: Outputs of Packing3D: Design for Sample B3.

3 Models

Two models are used in this study. The first (the Wave Propagation Model, or WPM) is an analytic, transmission-line model that predicts the surface impedance of a sample based on the geometry of the chambers. The second is an acoustic finite element model developed using COMSOL Multiphysics that predicts the surface impedance of a sample based on chamber geometry.

The WPM was used to design the samples [2, 4]. It employs a transmission line approach to calculate the sound pressure and particle velocity within each chamber. The model divides each chamber into two computational layers, the air cavity and the mesh facesheet [2, 5]. The backplate of the liner is assumed to be rigid, with an initial acoustic pressure p_0 of unity and particle velocity u_0 of zero, normalized by ρc^2 and c (air density and speed of sound in the test environment), respectively. Changes in these two values are then computed by

$$\begin{pmatrix} p_{n+1} \\ u_{n+1} \end{pmatrix} = \begin{pmatrix} T_{11} & T_{12} \\ T_{12} & T_{22} \end{pmatrix} \begin{pmatrix} p_n \\ u_n \end{pmatrix} \quad (1)$$

in which p_n and u_n are the acoustic pressure and particle velocity at the top of the n^{th} computational layer. The transmission coefficients T_{11} , T_{12} , and T_{22} are determined by the type of computational layer (air cavity or mesh, in this case). The normalized impedance ζ of a chamber with two computational layers is given by

$$\zeta = \frac{p_2}{u_2}.$$

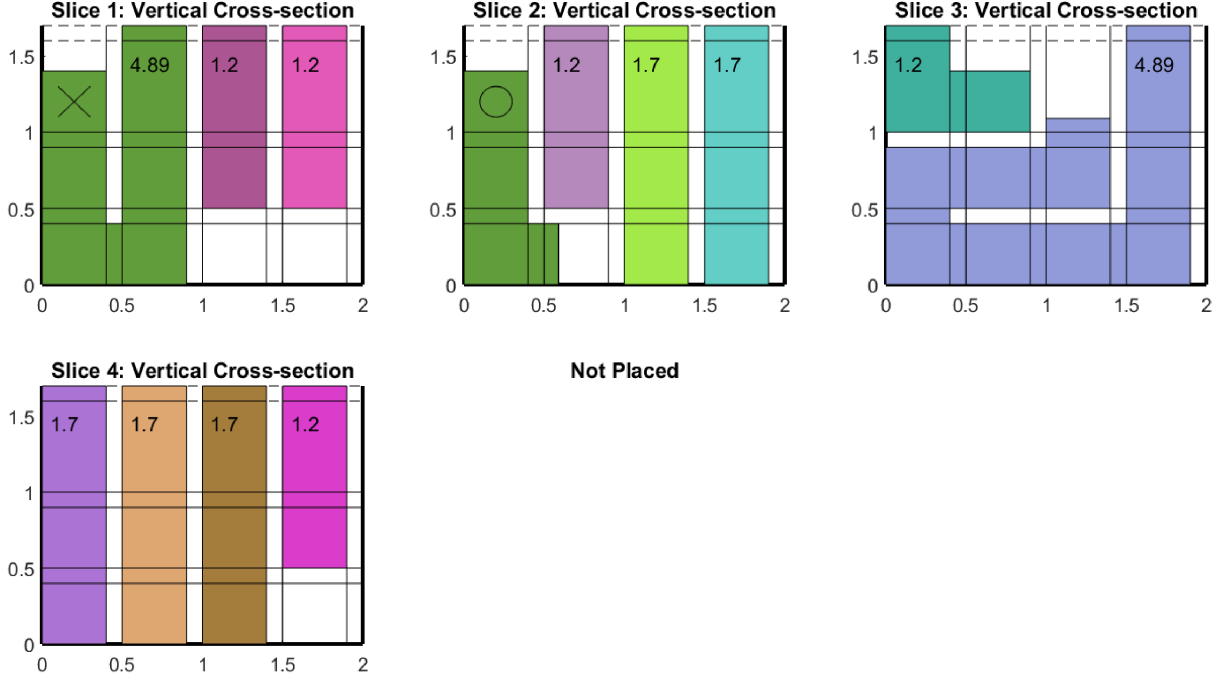


Figure 5: Outputs of Packing3D: Design for Sample B4_1.

The surface impedance of the liner is then found by combining the impedances of the separate chambers in the liner. The impedance is composed of resistance (θ) and reactance (χ) by the relation

$$\zeta = \theta + \chi i.$$

For an environment in which the sound is normally-incident on the sample surface, absorption (α) is used for comparison purposes and calculated from resistance and reactance as [5]

$$\alpha = \frac{4\theta}{(\theta + 1)^2 + \chi^2}.$$

It is important to note that this model does not take into account the shape or location of the chambers, only their lengths and cross-sectional areas.

The numerical model, by contrast, is more precise and inherently accounts for the shapes and locations of the chambers. This model was implemented using the Acoustics Module within COMSOL Multiphysics 5.2. As this method is more computationally intensive than the WPM, it is only used to create predictions for comparison to the measured data and is not part of the design process.

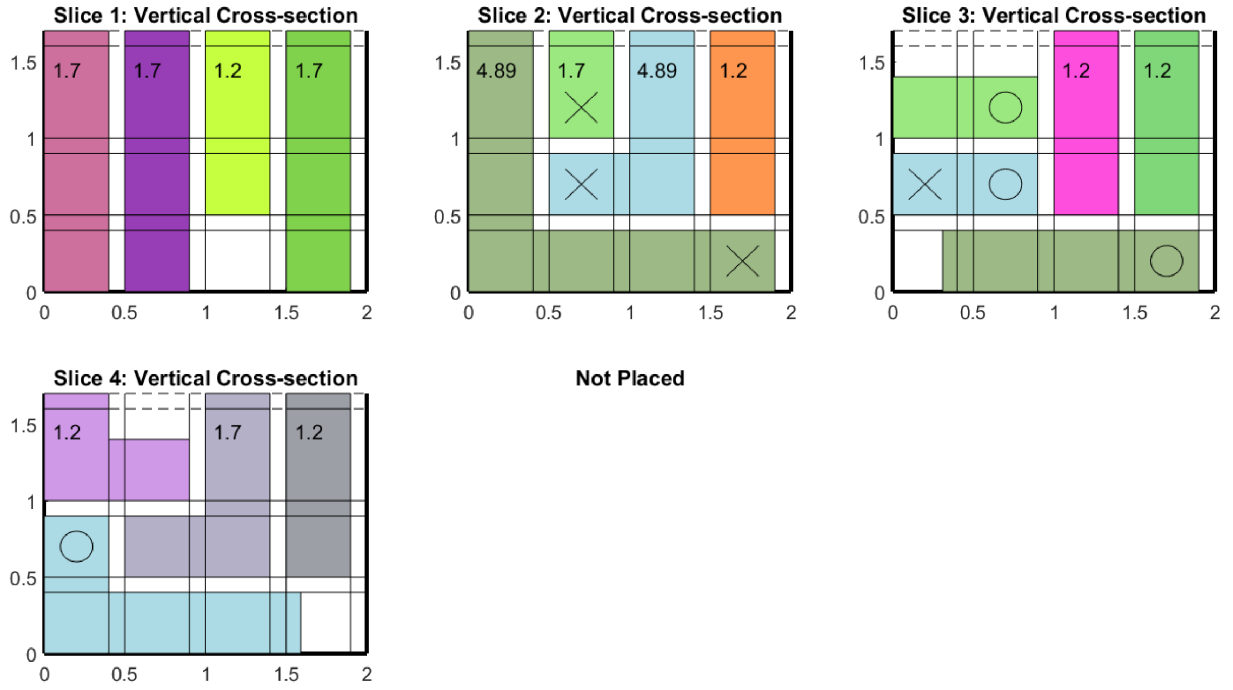


Figure 6: Outputs of Packing3D: Design for Sample B4_2.

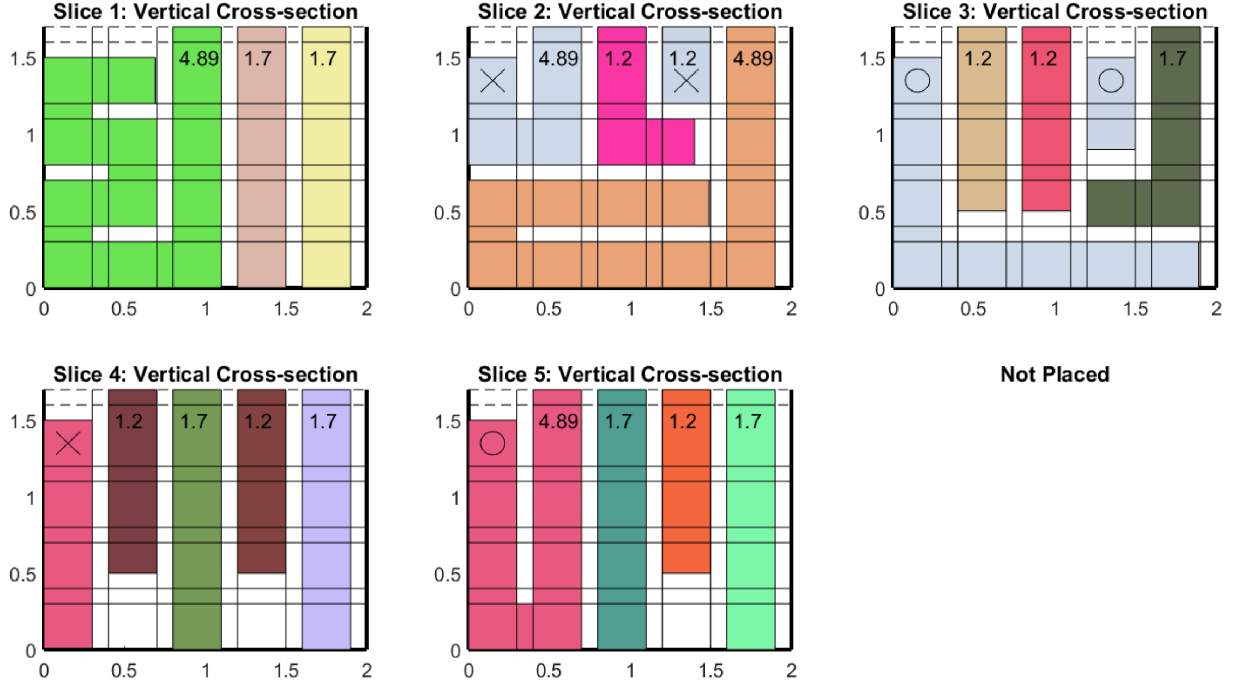


Figure 7: Outputs of Packing3D: Design for Sample B5.

4 Packing Code Evaluation

4.1 Sample Design

The general design goal for the four samples was to achieve an absorption spectrum with a peak at low frequencies (below 1 kHz), a dip around 1 kHz, and high broadband absorption at the higher frequencies (above 1 kHz). For the purposes of this study, the threshold between a “high” and “low” absorption was 0.5. The constraints on the samples are given in Table 1. The B5 sample was designed first, using an iterative approach. The chamber lengths and number of chambers of each length were varied until the absorption spectrum predicted by the WPM achieved the desired frequency-dependent pattern. For the sake of consistency, the chamber lengths in the subsequent samples were kept equal to the lengths used in the B5 sample and only the number of chambers was adjusted to best approximate the desired absorption spectrum.

Table 1: Constraints used in sample design.

Depth	1.7 in.
Active Area	2 in. x 2 in.
Thickness of Walls Between Chambers	0.1 in.
Frequency Viewing Range	400 - 3000 Hz.
Threshold Absorption	0.5

The distinguishing characteristics of the four samples (see Figs. 4 - 7) designed using the Packing3D code are given in Table 2. Three different chamber diameters are used to demonstrate the ability of the Packing3D code to handle different chamber widths as well as different levels of complexity in liner designs. Each of the four samples demonstrates a three-dimensional geometry. This means that a single chamber can bend along all three axes (i.e., bend normal to the plane). In Figure 4, this is visible where the longest chamber is bent in the plane of the page and then folds into the page to the next “slice” of the diagram.

Two samples, B4_1 and B4_2, have chambers of the same diameter. The difference in the design of these two samples is the use of different chamber placement algorithms. As described in Section 2, the code places chambers by checking adjacent cells for availability (see Fig. 3). In sample B4_1, the code prioritized the vertical plane and checked cells in the previous “row” (above the current cell) before checking those in the next or previous “slice”. In sample B4_2, the code prioritized the horizontal plane and checked cells in the next and previous slice before checking the previous row. This seemingly small difference resulted in a different style of chamber arrangement and enabled the available volume to be used more efficiently, as B4_2 contains one more chamber than B4_1. This demonstrates the flexibility of the code to be tailored to different circumstances. It also demonstrates the possibility of improving or optimizing the performance of the code.

Table 2: List of samples designed, built, and tested.

Sample	Chamber Width (in.)	Chamber Length (in.) (Number of Chambers)	Algorithm for cell choice
B3	0.567	4.89 (1), 1.7 (3), 1.2 (2)	Prioritize vertical plane
B4_1	0.4	4.89 (2), 1.7 (5), 1.2 (5)	Prioritize vertical plane
B4_2	0.4	4.89 (2), 1.7 (5), 1.2 (6)	Prioritize horizontal plane
B5	0.3	4.89 (4), 1.7 (7), 1.2 (7)	Prioritize vertical plane

When designing a relatively complex sample such as B5, which has 0.3 inch chambers and was designed on a 5 x 5 x 4 grid (similar to that in Figure 3), the Packing3D code had an average runtime of approximately 1-2 seconds. Less complex samples on the level of B4_1 and B4_2, which were designed on a 4 x 4 x 3 grid, required approximately 0.6 seconds to run, and the simplest sample (B3, on a 3 x 3 x 2 grid) required approximately 0.4 seconds. This is a drastic decrease from the minutes or hours that would be required to draft these designs by hand.

The samples were produced using 3D-printing stereolithography wherein the desired shapes are formed using a liquid plastic resin hardened by laser light [2, 6]. Each sample was tested in the NIT (Fig. 8), which is a waveguide that has a square cross-section with a side of two inches. This cross section determines the active area of the sample. Six acoustic drivers are placed at one end of the impedance tube and the sample at the other. There is no airflow. A swept-sine source was employed, allowing the data to be acquired at approximately 5 Hz intervals over the range of 400 to 3000 Hz [7]. The Two Microphone Method was then used to determine the impedance at the surface of the sample based on the acoustic pressures measured by two microphones mounted in the wall of the NIT [8]. Each sample was tested with and without a 27 cgs rayl mesh facesheet, and with a source sound pressure level of 120 dB (as measured by the reference microphone).

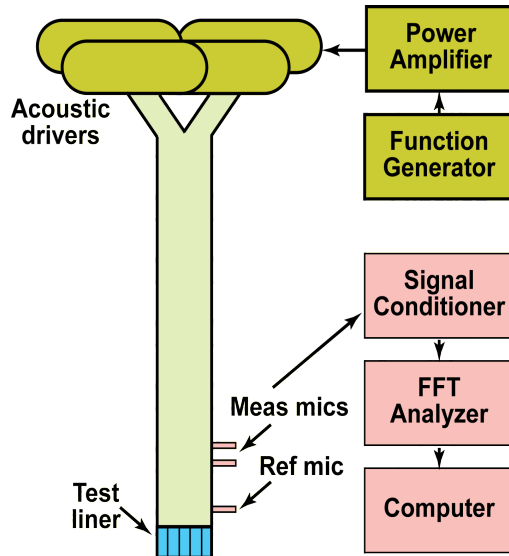


Figure 8: Normal Incidence Tube (NIT).

4.2 Results

Each of the samples depicted in Figures 4 - 7 was tested in the NIT with a source sound pressure level of 120 dB. The original design process conducted with the WPM assumed there was no facesheet, such that the resistance was confined to scrubbing losses along the interior walls of the variable-depth chambers. However, these configurations would not be suitable for use in a flow duct application (e.g., mounted in the interior walls of an aircraft engine nacelle) without a facesheet, so tests were also conducted with a 270 MKS Rayl wire mesh facesheet. The addition of the wire mesh causes the total resistance to increase at the surface of the liner.

Results for the least (B3) and most (B5) complex configurations with no facesheet are presented in Figure 9, while the corresponding results with the addition of a wire mesh facesheet are provided in Figure 10. These figures present comparisons of absorption coefficient spectra measured in the NIT and predicted with COMSOL.

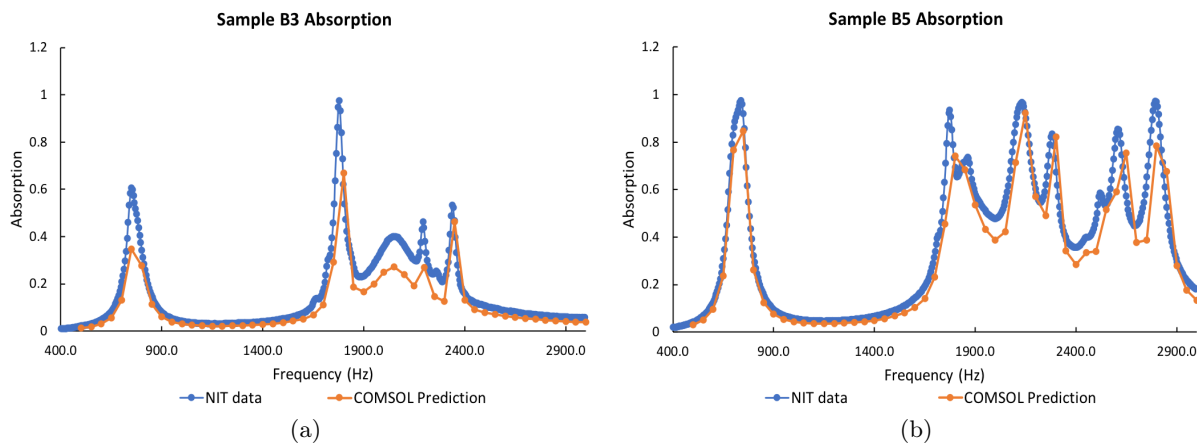


Figure 9: Absorption data for Samples B3 (9a) and B5 (9b), tested without mesh.

For both samples tested without a facesheet, the measured data (blue) match the COMSOL predictions (orange) very closely. The remaining two samples have similar absorption spectra and a similar favorable comparison. These results demonstrate that the liner configurations were able to achieve good absorption at the lower frequency target, while providing broadband absorption over the higher frequency range. However, the B3 configuration was able to achieve an absorption coefficient of at least 0.5 at just a few frequencies in the higher range. The broadband high frequency results for the B5 configuration are more promising, as the absorption coefficient is above 0.5 for a significant portion of the high frequency range.

In both cases, the limiting feature was the resistance, i.e., there is insufficient resistance achieved via the scrubbing losses in the interior walls. As expected, the addition of the wire mesh facesheet improves these results. In Figure 10, the threshold absorption of 0.5 is shown in black, the measured data in blue, and two COMSOL predictions in orange and yellow. The low frequency peak and higher frequency broadband absorption are both clearly visible in the measured data. The additional

resistance causes the measured absorption coefficient to remain above 0.5 for the majority of the frequency range of the test, with significant absorption at the design frequencies. This is the case for all four samples.

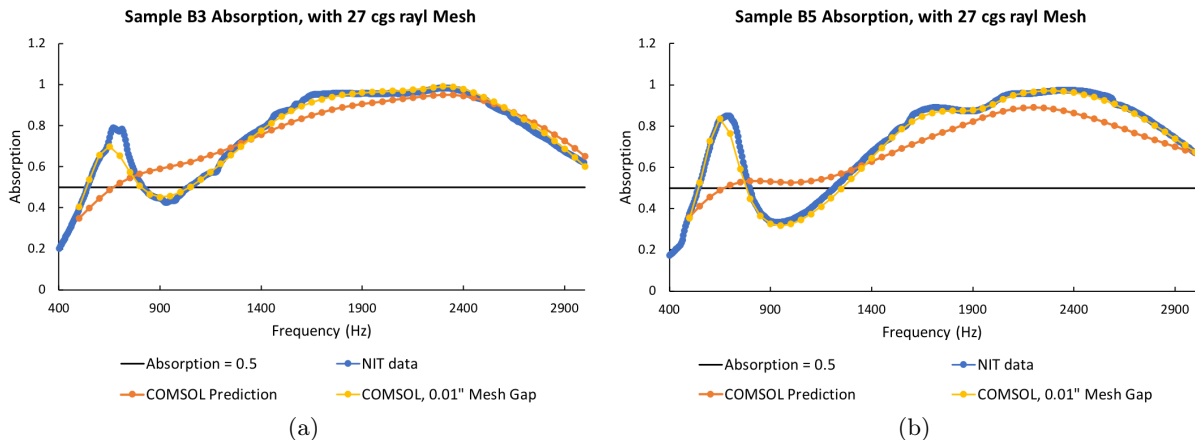


Figure 10: Absorption data for Samples B3 (10a) and B5 (10b), tested with a 27 cgs rayl mesh facesheet.

The original COMSOL predictions (orange curve) capture the general trends of the B3 and B5 samples, but fail to predict the detailed features of the measured absorption coefficient spectra. A closer look at Figures 9b and 10b indicates that the large low frequency discrepancy between the measured and predicted absorptions for sample B5 is only present in the mesh case. This pattern holds for all four samples.

One possible cause for this discrepancy is the way in which the mesh is mounted onto the core. As the mesh is only attached at the edges of the sample, it is possible for the mesh to become separated from the sample in the interior. This would enable acoustic interactions below the mesh between adjacent chambers, especially between those of different lengths. The additional COMSOL prediction (yellow curve in Figure 10) assumes an 0.01” gap between the mesh and sample, resulting in a better match between predictions and measurements. While this does not prove that there is indeed an 0.01” gap, it does imply that mesh separation may be the cause for the discrepancy.

5 Concluding Remarks

The results demonstrate the ability of the Packing3D code to quickly design chamber configurations in samples that fit the predetermined goals and constraints. Furthermore, the results indicate that the liner samples are performing as predicted when there is no facesheet. Although there is a visible discrepancy between the measured and predicted data when a mesh is added to the surface of the samples, there is evidence that this discrepancy may be caused by a separation between the mesh and the sample core, and not by an error in the sample design. The adherence to the predicted absorption trends implies that the samples are built based on designs with the correct chamber dimensions. This information supports the assertion that the Packing3D MATLAB code can reliably create successful, predictable designs and package a given set of chambers with a square

cross-section into an NIT sample of limited volume.

The packaging process is quick, accurate, and allows for complexity that would be difficult and time-consuming in designs done by hand. Furthermore, the Packing3D code can be adjusted to address a broader range of design situations using the same basic algorithm. It can also be used as a starting point for an optimizer, as the random element in the chamber placement and the way that the information is stored lend themselves to optimization. The code could be used to package given chambers into the smallest volume possible with relatively few adjustments.

References

1. Lockard, D. P. and Lilley, G. M., “The Airframe Noise Reduction Challenge,” NASA TM 213013, 2004.
2. M. G. Jones, B. M. Howerton, E. A., “Evaluation of Parallel-Element, Variable-Impedance, Broadband Acoustic Liner Concepts,” AIAA Paper 2012-2194, June 2012.
3. Brian M. Howerton, Michael G. Jones, J. L. B., “Development and Validation of an Interactive Liner Design and Impedance Modeling Tool,” AIAA Paper 2012-2197, 2012.
4. M. G. Jones, D. M. Nark, A. B. and Smith, C. R., “Applications of Parallel-Element, Embedded Mesh-Cap Acoustic Liner Concepts,” AIAA Paper 2018-3445, June 2018.
5. Tony L. Parrott, M. G. J., “Parallel-element liner impedances for improved absorption of broadband sound in ducts,” *Noise Control Engineering Journal*, Vol. 43, No. 6, 1995, pp. 183–195.
6. Noah H. Schiller, M. G. J., “Smearred Impedance Model for Variable Depth Liners,” AIAA Paper 2018-3774, June 2018.
7. Howerton, B. M., Vold, H., and Jones, M. G., “Application of Sine Sweep Excitation for Acoustic Impedance Education,” AIAA Paper 2019-2487, May 2019.
8. Michael G. Jones, T. L. P., “Evaluation of a Multi-point Method for Determining Acoustic Impedance,” *Mechanical Systems and Signal Processing*, Vol. 3, No. 1, 1989, pp. 15–35.
9. Schiller, N. H., Jones, M. G., and Bertolucci, B., “Experimental Evaluation of Acoustic Engine Liner Models Developed with COMSOL Multiphysics,” AIAA Paper 2017-4186, June 2017.

REPORT DOCUMENTATION PAGE			Form Approved OMB No. 0704-0188		
<p>The public reporting burden for this collection of information is estimated to average 1 hour per response, including the time for reviewing instructions, searching existing data sources, gathering and maintaining the data needed, and completing and reviewing the collection of information. Send comments regarding this burden estimate or any other aspect of this collection of information, including suggestions for reducing this burden, to Department of Defense, Washington Headquarters Services, Directorate for Information Operations and Reports (0704-0188), 1215 Jefferson Davis Highway, Suite 1204, Arlington, VA 22202-4302. Respondents should be aware that notwithstanding any other provision of law, no person shall be subject to any penalty for failing to comply with a collection of information if it does not display a currently valid OMB control number.</p> <p>PLEASE DO NOT RETURN YOUR FORM TO THE ABOVE ADDRESS.</p>					
1. REPORT DATE (DD-MM-YYYY) 01-02-2020		2. REPORT TYPE Technical Memorandum		3. DATES COVERED (From - To)	
4. TITLE AND SUBTITLE Evaluation of Packing_3D Code for Design of Variable-Depth, Bent-Chamber Acoustic Liners			5a. CONTRACT NUMBER		
			5b. GRANT NUMBER		
			5c. PROGRAM ELEMENT NUMBER		
6. AUTHOR(S) Marinova, Miroslava M.; Jones, Michael G.; Schiller, Noah H.			5d. PROJECT NUMBER		
			5e. TASK NUMBER		
			5f. WORK UNIT NUMBER 081876.02.07.12.01.02		
7. PERFORMING ORGANIZATION NAME(S) AND ADDRESS(ES) NASA Langley Research Center Hampton, Virginia 23681-2199			8. PERFORMING ORGANIZATION REPORT NUMBER L-21109		
9. SPONSORING/MONITORING AGENCY NAME(S) AND ADDRESS(ES) National Aeronautics and Space Administration Washington, DC 20546-0001			10. SPONSOR/MONITOR'S ACRONYM(S) NASA		
			11. SPONSOR/MONITOR'S REPORT NUMBER(S) NASA/TM-2020-220560		
12. DISTRIBUTION/AVAILABILITY STATEMENT Unclassified-Unlimited Subject Category 71 Availability: NASA STI Program (757) 864-9658					
13. SUPPLEMENTARY NOTES An electronic version can be found at http://ntrs.nasa.gov .					
14. ABSTRACT Increases in commercial aircraft engine bypass ratios have caused broadband fan noise to become dominant. Thus, acoustic liners are needed for absorption of fan noise over a wide frequency range. Variable depth liners with three-dimensional bent chambers present one way to achieve this goal but can be difficult to design. A packing code, Packing3D, was developed to design chamber configurations of such liners once the chamber dimensions and volume constraints are known. It uses a randomized trial and error approach to place each chamber, then returns information needed to fabricate the liner. For evaluation, the code is used to design four liners of varying levels of complexity. These liners are tested in the NASA Langley Normal Incidence Tube, and the results are compared to COMSOL predictions. The results indicate the packing code is able to quickly design samples that are predictable, achieve the desired absorption spectrum, and fit the given constraints. This code is flexible, lends itself to optimization, and allows samples to be designed quickly, accurately, and efficiently.					
15. SUBJECT TERMS acoustic, liner, packing					
16. SECURITY CLASSIFICATION OF:			17. LIMITATION OF ABSTRACT	18. NUMBER OF PAGES	19a. NAME OF RESPONSIBLE PERSON
a. REPORT	b. ABSTRACT	c. THIS PAGE			STI Information Desk (help@sti.nasa.gov)
U	U	U	UU	17	19b. TELEPHONE NUMBER (Include area code) (757) 864-9658